

Thermo-physical properties, excess and deviation properties for a mixture of γ -butyrolactone with diethyl carbonate or propylene carbonate

Kyeong-Ho Lee and So-Jin Park[†]

Department of Chemical Engineering, College of Engineering, Chungnam National University, Daejeon 34134, Korea
(Received 24 July 2017 • accepted 18 September 2017)

Abstract—The paper reports the thermodynamic and transport properties of the materials that are used in liquid electrolytes of lithium ion batteries (LIBs). Linear and cyclic carbonates are commonly used solvents for organic electrolyte solutions. On the other hand, γ -butyrolactone (GBL) could also be an attractive solvent because it has sufficiently high permittivity to dissociate lithium salts. This prompted us to investigate the thermo-physical properties such as the density, refractive index, kinematic viscosity (298.2 to 328.2 K) and the excess and deviation properties (298.2 to 318.2 K) for a mixture of GBL and diethyl carbonate (DEC) or propylene carbonate (PC). The thermo-physical properties, i.e., the density, refractive index, and kinematic viscosity, were correlated by employing DIPPR, and linear and Goletz/Tassion equations, respectively. The excess and deviation properties were computed and modeled by the polynomial Redlich-Kister equations for each of the binary fractions.

Keywords: γ -Butyrolactone, Excess Property, Deviation Property, Density, Viscosity

INTRODUCTION

Lithium is the most electropositive and the lightest metal. Thus, lithium ion batteries (LIBs) have the potential to provide high energy density and high specific current capacity. These batteries are considered the most promising rechargeable form of energy storage and are therefore used in various applications, e.g., as power source for electric vehicles and as storage for electric energy generated by solar and wind energy sources [1,2]. The three basic parts of LIBs that have been the focus of interest are the anode, cathode, and electrolyte. However, the energy stored in the electrodes in LIBs requires them to work together with a lithium conducting liquid or solid electrolyte. Some characteristics of LIBs, such as their lifetime, specific power, and good performance at low and high temperature are largely dependent on the electrolyte or, more specifically, a suitable combination of electrolytes.

A liquid electrolyte generally consists of a lithium salt, usually LiPF_6 or $\text{LiN}(\text{CF}_3\text{SO}_2)_2$ and an organic solvent blend of linear and cyclic alkyl carbonates. The selection of the components of the solvent mixture is therefore a crucial aspect for enhancing the performance of LIBs. In practice, this solvent mixture is mainly composed of ethylene carbonate (EC) and propylene carbonate (PC) with one or more co-solvents such as dimethyl carbonate (DMC), diethyl carbonate (DEC), and ethyl methyl carbonate (EMC). As another electrolyte in LIBs, LiBF_4 has several advantages compared to more common LiPF_6 , such as relatively high thermal stability and moisture tolerance. As a matter of interest, γ -butyrolactone (GBL) is a very attractive solvent for LiBF_4 because it enhances the relatively low conductivity of LiBF_4 and has high permittivity to

dissociate lithium salts. In addition, GBL is advantageous from a safety point of view by comparison with some of the linear carbonates, which have both low boiling and low flashing points [3,4].

Determination of thermo-physical properties and excess and deviation properties according to the temperature and compositions is a crucial part to study interactions between components of electrolyte solution. Therefore, we have systematically measured physical and excess thermodynamic properties for binary or ternary electrolyte mixtures. In the present work, we determined the physical properties, density, refractive index and kinematic viscosity at different temperatures from 298.2 K to 323.2 K, and calculated the excess volume and deviation properties of the refractive indices and kinematic viscosity at 298.2 K, 308.2 K, and 318.2 K for mixtures of GBL with either DEC or PC. Our work was motivated by the fact that a good understanding of the thermodynamic and transport properties of GBL-containing mixtures as co-solvent of LIBs is very useful and can be expected to be helpful in their utilization as electrolytes [5,6].

The thermodynamic properties of binary mixtures of GBL were previously investigated by researchers such as Chen et al. [7], Ritzoulis et al. [8], Lu et al. [9], and Huang et al. [10]. However, as far as our present knowledge goes, the experimental thermo-physical properties for the systems considered in this work have not yet been reported.

The determined density, refractive index, and kinematic viscosity were correlated with DIPPR [11,12], linear [11], and Goletz/Tassion equations [11,13], respectively. The excess and deviation properties were computed and modeled by polynomial equations, namely the Redlich-Kister equations for binary fractions [14].

EXPERIMENTAL SECTION

1. Materials

GBL and EC were provided by Samchun Chemical (Korea).

[†]To whom correspondence should be addressed.

E-mail: sjpark@cnu.ac.kr

Copyright by The Korean Institute of Chemical Engineers.

Table 1. Comparison of physical properties at 298.2 K

Chemicals	$\rho/\text{g}\cdot\text{cm}^{-3a}$		n_D^b		$\nu/\text{mm}^2\cdot\text{s}^{-1c}$	
	Exp.	Lit.	Exp.	Lit.	Exp.	Lit.
GBL	1.12456	1.12426 ²	1.4351	1.4356 ³	1.466	1.54 ²
DMC	1.06328	1.06295 ⁴	1.3663	1.3664 ⁵	0.539	0.5429 ⁴
DEC	0.96937	0.96897 ⁶	1.3822	1.38240 ⁷	0.734	0.770 ⁶
EMC	1.00691	-	1.3752	-	0.618	-
EC ¹	1.32135	1.321991 ⁸	1.4192	1.4195 ⁹	1.388	1.421 ⁸
PC	1.19935	1.19902 ¹⁰	1.4197	1.4194 ¹¹	1.979	2.21 ¹⁰

¹The property for EC was at 313.2 K. ²Ref. 12, ³Ref. 13, ⁴Ref. 14, ⁵Ref. 15, ⁶Ref. 16, ⁷Ref. 17, ⁸Ref. 18, ⁹Ref. 19, ¹⁰Ref. 20, ¹¹Ref. 21

^aStandard uncertainties u are $u(\rho)=6\times 10^{-5}\text{ g}\cdot\text{cm}^{-3}$, $u(T)=0.01\text{ K}$

^bStandard uncertainties u are $u(n_D)=1.5\times 10^{-4}$, $u(T)=0.05\text{ K}$

^cStandard uncertainties u are $u(\nu)=0.001\text{ mm}^2\cdot\text{s}^{-1}$, $u(T)=0.01\text{ K}$. The range of the Ubbelohde viscometer utilized in this experiment was approximately 0.5 to $3\text{ mm}^2\cdot\text{s}^{-1}$

DMC and DEC were supplied by Acros Organics (USA), while EMC and PC were purchased from Sigma Aldrich (USA). The purities of all the chemicals were greater than 99.9 mass%, as determined by GC analysis. All the chemicals were dried with 0.3 nm molecular sieves and used without further purification. The water content of all the chemicals was checked using a Karl-Fischer titrator (Metrohm 684 KF-Coulometer) and showed less than $5\times 10^{-5}\text{ g}\cdot\text{g}^{-1}$ for all the chemicals. The determined physical properties and reported literature values of the chemicals are listed in Table 1 [15-24].

2. Apparatus and Procedure

The densities (ρ) of the pure and mixed components at atmospheric pressure were measured on a vibrating tube densitometer (Anton Paar model DMA 5000). This method automatically eliminated long-term drift by a reference oscillator built into the measuring cell and allowed for a full-range viscosity correction. The temperature of the U-tube in the densitometer was determined by a high-precision platinum resistance probe with an accuracy of 0.01 K. The densitometer was calibrated automatically by measuring the densities of atmospheric air and bi-distilled water. The experimental procedure has been described in detail elsewhere [25,26]. Approximately 3 ml sample mixtures were prepared in narrow-mouth stoppered glass vials by adding the heavier component first to minimize evaporation losses using a microbalance (OHAUS Co. DV215CD) with a precision of $1\times 10^{-5}\text{ g}$. These sample mixtures were used both for the density and refractive index measurements. The experimental systematic error in the mass measurements

was estimated to be less than 1×10^{-4} in the mole fraction.

The kinematic viscosity (ν) was measured directly using an Ubbelohde viscometer and an automatic measuring unit (LAUDA, model PVS1, Germany) with a precision thermostat. The accuracy of the flowing time measurement was 0.01 s and the temperature of the thermostat regulated with an accuracy of $\pm 0.01\text{ K}$. The samples in the viscometer, which was submerged in a thermostat bath, were kept there for more than 30 min to attain thermal equilibrium. Then, we carefully recorded the flowing time of the sample through the capillary tube of the viscometer. The measurement was repeated three times and the average value was taken as the flowing time. The measurement range of the Ubbelohde viscometer was approximately 0.5 to $3,000\text{ mm}^2\cdot\text{s}^{-1}$ [27].

The refractive indexes (n_D) of the pure components and mixtures were measured using a KEM model RA-520N digital precision refractometer, manufactured from Kyoto, Japan. The measurement was carried out three times and the average values were adopted. The experimental procedure has been described in detail elsewhere [28].

RESULTS AND DISCUSSION

1. Physical Properties

The physical properties--densities, refractive indices, and kinematic viscosities--that were measured from 298.2 K to 323.2 K are listed in Tables 2 through 4, respectively. However, in the case of

Table 2. Densities ρ ($\text{g}\cdot\text{cm}^{-3}$) for chemicals used at 298.2 K-323.2 K

Temperature	$\rho/\text{g}\cdot\text{cm}^{-3a}$					
	GBL	DMC	DEC	EMC	EC	PC
298.2 K	1.12456	1.06328	0.96937	1.00691	-	1.19935
303.2 K	1.11967	1.05666	0.96355	1.00086	-	1.19407
308.2 K	1.11477	1.05002	0.95809	0.99479	-	1.18879
313.2 K	1.10987	1.04339	0.95239	0.98869	1.32135	1.18343
318.2 K	1.10498	1.03665	0.94676	0.98256	1.31569	1.17819
323.2 K	1.10005	1.02991	0.94089	0.97640	1.30994	1.17291

^aStandard uncertainties u are $u(\rho)=6\times 10^{-5}\text{ g}\cdot\text{cm}^{-3}$, $u(T)=0.01\text{ K}$

Table 3. Refractive indices n_D for each component at 298.2-323.2 K

Temperature	n_D^a					
	GBL	DMC	DEC	EMC	EC	PC
298.2 K	1.4351	1.3663	1.3822	1.3752	-	1.4197
303.2 K	1.4331	1.3638	1.3801	1.3730	-	1.4180
308.2 K	1.4310	1.3617	1.3776	1.3707	-	1.4157
313.2 K	1.4288	1.3592	1.3754	1.3686	1.4192	1.4134
318.2 K	1.4266	1.3570	1.3730	1.3664	1.4173	1.4118
323.2 K	1.4244	1.3546	1.3709	1.3643	1.4154	1.4099

^aStandard uncertainties u are $u(n_D)=1.5 \times 10^{-4}$, $u(T)=0.05$ K

Table 4. Kinematic viscosities ν ($\text{mm}^2 \cdot \text{s}^{-1}$) for each component at 298.2-323.2 K

Temperature	$\nu/\text{mm}^2 \cdot \text{s}^{-1a}$					
	GBL	DMC	DEC	EMC	EC	PC
298.2 K	1.466	0.539	0.734	0.618	-	1.979
303.2 K	1.350	0.514	0.693	0.585	-	1.809
308.2 K	1.274	0.488	0.655	0.555	-	1.659
313.2 K	1.189	0.461	0.621	0.526	1.388	1.526
318.2 K	1.114	0.440	0.591	0.501	1.287	1.412
323.2 K	1.050	0.421	0.563	0.479	1.201	1.312

^aStandard uncertainties u are $u(\nu)=0.001 \text{ mm}^2 \cdot \text{s}^{-1}$, $u(T)=0.01$ K. The range of the Ubbelohde viscometer utilized in this experiment was approximately 0.5 to $3 \text{ mm}^2 \cdot \text{s}^{-1}$

EC, we determined the aforementioned properties above the temperature of 313.2 K because of the extremely high melting temperature of EC. The experimental standard deviation for each physical property, $s(X)$, for an unbiased sample deviation was calculated by using Eq. (1). Furthermore, the type A standard uncertainty of the measurement of these properties, $u(\bar{X})$, was calculated from Eq. (2).

$$s(X) = \sqrt{\frac{\sum_i^N (X_i - \bar{X})^2}{N-1}} \quad (1)$$

$$u(\bar{X}) = \sqrt{\frac{\sum_i^N (X_i - \bar{X})^2}{N(N-1)}} \quad (2)$$

where X_i is the experimental value of the component i , \bar{X} is the average of multiple experimental value, and N is the number of experimental points. The standard uncertainty in this work is the Type A and specifically refers to repeatability. The probability of uncertainty has 0.68 level of confidence.

The standard uncertainty for the density (ρ) measurement was calculated to be less than $u(\rho)=6 \times 10^{-5} \text{ g} \cdot \text{cm}^{-3}$ and the standard uncertainty of the refractive indices ($u(n_D)$) was estimated to be less than 1.5×10^{-4} according to Eq. (2). In the case of the kinematic viscosity (ν), the standard deviation was calculated by multiplying the viscometer constant by the efflux time as an experimental property. The estimated averaged standard uncertainty ($u(\nu)$) was calculated to be less than ($u(\nu)$)= $0.001 \text{ mm}^2 \cdot \text{s}^{-1}$ (cSt).

Fig. 1 through 3 illustrates the pure component properties--densities, refractive indices, and kinematic viscosities--from 298.2 K to 323.2 K with the recalculated values (solid lines) from each cor-

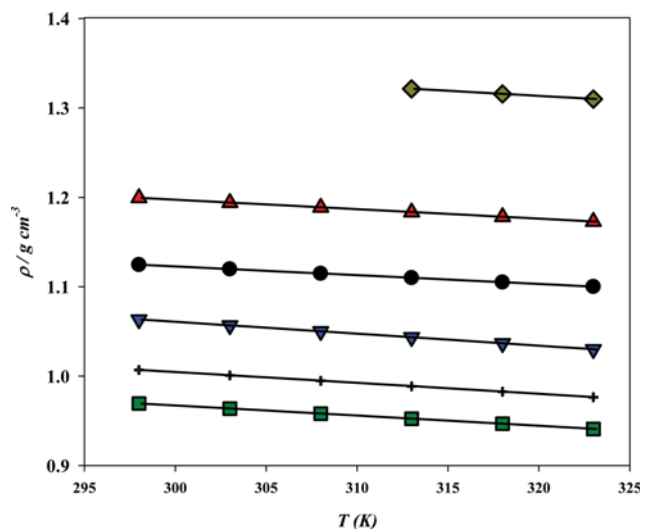


Fig. 1. Densities ρ ($\text{g} \cdot \text{cm}^{-3}$) for 298.2-323.2 K; (●), GBL; (▼), DMC; (■), DEC; (★), EMC; (◆), EC; (▲), PC; solid curves were calculated from DIPPR equation.

related model equation parameters.

For the correlation of the densities, the DIPPR (Daubert and Danner) model [11,12] was used to fit the data.

$$\rho/\text{g} \cdot \text{cm}^{-3} = a/[b^{1+(T/K)/c}]^d \quad (3)$$

where a , b , c , and d are regressible parameters. The regression of the parameters was carried out by iteratively performing the calculation and taking the parameters that gave the minimum value of

Table 5. Fitted parameters for DIPPR, linear, and Goletz and Tassion equations and standard deviations for each component

Chemical	DIPPR					Linear			Goletz and Tassion			
	a	b	c	d	σ_{st}	I	S	σ_{st}	A	B	C	σ_{st}
GBL	0.3433	0.4943	620.31	0.5791	1.8×10^{-5}	1.5626	-4.3×10^{-4}	1.0×10^{-4}	0.0168	1363.8	0.0082	0.0081
DMC	0.1568	0.3303	591.29	0.4528	4.2×10^{-5}	1.5047	-4.6×10^{-4}	8.2×10^{-5}	1.2×10^{-4}	1092.0	4.7995	0.0019
DEC	0.1522	0.3446	593.13	0.4351	1.4×10^{-5}	1.5193	-4.6×10^{-4}	9.8×10^{-5}	1.9×10^{-4}	1139.7	4.4323	6.5×10^{-4}
EMC	0.2777	0.4581	501.75	0.4772	3.9×10^{-5}	1.5059	-4.4×10^{-4}	6.3×10^{-5}	4.1×10^{-4}	1110.6	3.5971	6.4×10^{-4}
EC	0.4726	0.5371	556.09	0.5126	1.7×10^{-5}	1.5377	-3.7×10^{-4}	3.1×10^{-5}	0.0490	1555.4	-1.3459	0.0018
PC	0.5869	0.6135	515.19	0.7420	5.0×10^{-5}	1.5358	-3.9×10^{-4}	1.6×10^{-4}	0.0061	1679.2	0.3388	0.0047

standard deviation from the experimental data. The fitted parameters are listed in Table 5 with their corresponding standard deviations of the fit, σ_{st} , defined as:

$$\sigma_{st} = \sqrt{\frac{\sum_i^N (X_i^{calc} - X_i^{exp})^2}{(N-n)}} \quad (4)$$

where X_i^{calc} and X_i^{exp} are the calculated and experimental value of component i , respectively, N is the number of experimental points, and n is the number of fitted parameters. In the correlation of the experimental density in Table 5, the σ_{st} values obtained by the DIPPR model were less than 5.0×10^{-5} for all of the tested compounds. A comparison of the experimental density with the recalculated data from the correlated parameters for each of the chemicals is shown in Fig. 1 from 298.2 K to 323.2 K except for EC, which starts at 313.2 K. As shown in Fig. 1, the DIPPR model correlated the experimental density very well. DEC showed the lowest standard deviation of $\sigma_{st} = 1.4 \times 10^{-5}$, whereas PC showed the largest deviation of 5.0×10^{-5} . The determined n_D were correlated with a following linear equation [11]:

$$n_D = I + S \cdot (T/K) \quad (5)$$

The adjustable parameters, I and S with standard deviation (σ_{st})

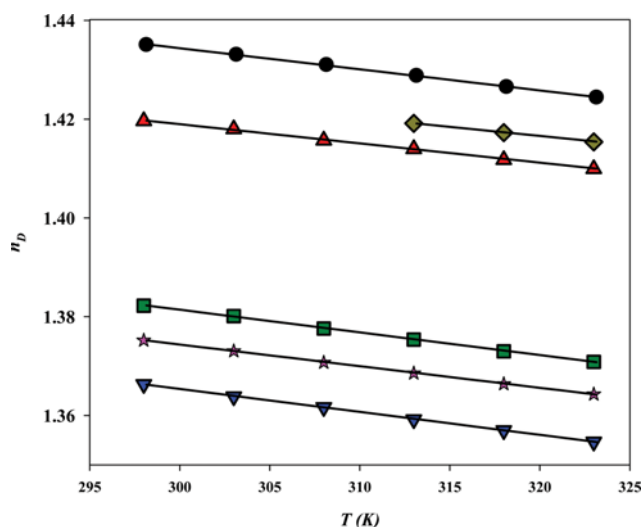


Fig. 2. Refractive indices n_D for 298.2–323.2 K; (●), GBL; (▼), DMC; (■), DEC; (★), EMC; (◆), EC; (▲), PC; solid curves were calculated from linear equation.

are listed in Table 5. As illustrated in Fig. 2, this linear relation was satisfactorily fitted to the experimental values as a function of temperature. The σ_{st} values between the experimental and calculated data were at least less than 1.6×10^{-4} . The largest deviation value of 1.6×10^{-4} was shown in PC, whereas EC showed the smallest deviation of 3.1×10^{-5} . Meanwhile, experimental ν were correlated with the following Goletz and Tassion Eq. [11,13]:

$$\nu / \text{mm}^2 \text{ s}^{-1} = A e^{[B/(T/K)+C]} \quad (6)$$

The adjustable Goletz and Tassion parameters A , B , and C with standard deviations are also provided in Table 5. As shown in Table 5, the Goletz and Tassion equation correlates well experimental data within ca. 0.8% of the mean deviations. Fig. 3 shows the experimental kinematic viscosity with the recalculated values from the correlated Goletz and Tassion parameters. Among the calculated standard deviations, GBL showed the maximum deviation of 0.0081, whereas EMC showed the smallest deviation of 6.4×10^{-4} .

2. Excess and Deviation Properties

The physical properties of the binary mixtures in the form of the measured density, refractive indices, and kinematic viscosity for {DEC(1)+GBL(2)} and {PC(1)+GBL(2)} are listed in Tables 6–9, along with the calculated excess molar volume (V^E), the devia-

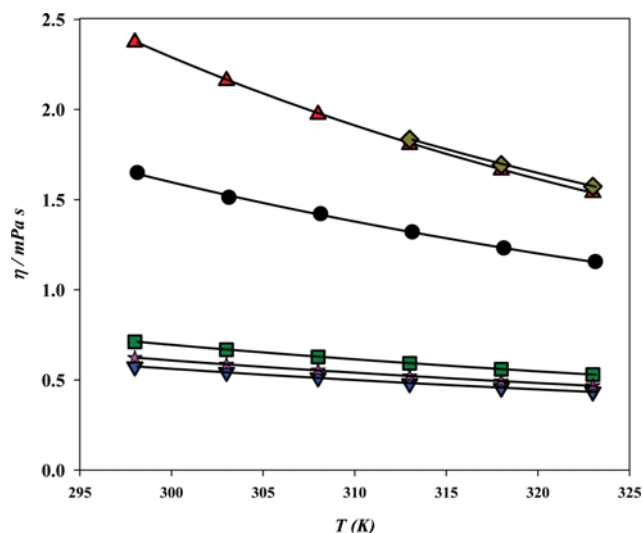


Fig. 3. Kinematic viscosities ν ($\text{mm}^2 \cdot \text{s}^{-1}$) for 298.2–323.2 K; (●), GBL; (▼), DMC; (■), DEC; (★), EMC; (◆), EC; (▲), PC; solid curves were calculated from Goletz and Tassion equation.

Table 6. Densities, excess molar volumes, refractive indices, and deviations in molar refractivity for diethyl carbonate(1)+ γ -butyrolactone(2) binary systems at 298.2-318.2 K

x_1	$\rho/\text{g cm}^{-3a}$	$V^E/\text{cm}^3 \text{mol}^{-1}$	n_D^b	$\Delta R/\text{cm}^3 \text{mol}^{-1}$
298.2 K				
0.0500	1.11407	-0.1070	1.4315	-0.3204
0.0995	1.10408	-0.2001	1.4282	-0.5875
0.1996	1.08495	-0.3531	1.4217	-0.9955
0.2999	1.06709	-0.4607	1.4157	-1.2398
0.3988	1.05073	-0.5295	1.4102	-1.3500
0.4941	1.03590	-0.5531	1.4051	-1.3474
0.5976	1.02078	-0.5363	1.3999	-1.2395
0.6998	1.00670	-0.4724	1.3951	-1.0373
0.7997	0.99368	-0.3647	1.3907	-0.7589
0.8980	0.98145	-0.2146	1.3864	-0.4208
0.9498	0.97533	-0.1197	1.3843	-0.2146
308.2 K				
0.0496	1.10430	-0.1128	1.4273	-0.3302
0.1000	1.09406	-0.2168	1.4241	-0.5966
0.1979	1.07519	-0.3771	1.4179	-0.9898
0.2988	1.05713	-0.4981	1.4118	-1.2389
0.3902	1.04175	-0.5627	1.4066	-1.3452
0.4897	1.02594	-0.5800	1.4013	-1.3447
0.6002	1.00979	-0.5791	1.3956	-1.2391
0.7010	0.99579	-0.5119	1.3910	-1.0228
0.7981	0.98282	-0.3822	1.3864	-0.7524
0.8970	0.97051	-0.2322	1.3820	-0.4199
0.9474	0.96440	-0.1311	1.3798	-0.2250
318.2 K				
0.0497	1.09439	-0.1205	1.4235	-0.3034
0.0999	1.08411	-0.2293	1.4204	-0.5622
0.1999	1.06481	-0.4145	1.4144	-0.9529
0.2990	1.04693	-0.5404	1.4083	-1.2041
0.3942	1.03081	-0.6142	1.4030	-1.3003
0.4999	1.01402	-0.6420	1.3972	-1.3031
0.5974	0.99951	-0.6239	1.3919	-1.2114
0.6974	0.98545	-0.5577	1.3868	-1.0322
0.7977	0.97201	-0.4296	1.3821	-0.7526
0.9007	0.95892	-0.2466	1.3774	-0.3997
0.9433	0.95365	-0.1493	1.3756	-0.2291

^aStandard uncertainties u are $u(x)$ 0.0001, $u(\rho)=6\times 10^{-5} \text{ g}\cdot\text{cm}^{-3}$, $u(T)=0.01 \text{ K}$

^bStandard uncertainties u are $u(n_D)=1.5\times 10^{-4}$, $u(T)=0.05 \text{ K}$

tions of the refractive indices (ΔR) and kinematic viscosity ($\Delta \nu$) for different temperatures of 298.2 K, 308.2 K, and 318.2 K. All of these physical properties, i.e., the determined density, refractive index, and kinematic viscosity, decreased with increasing temperatures for both binary systems. However, the temperature dependence of the excess and deviation properties were not exactly the same. The V^E values were calculated using Eq. (7) [29,30], which is as follows:

Table 7. Densities, excess molar volumes, refractive indices, and deviations in molar refractivity for propylene carbonate(1)+ γ -butyrolactone(2) binary systems at 298.2-318.2 K

x_1	$\rho/\text{g cm}^{-3a}$	$V^E/\text{cm}^3 \text{mol}^{-1}$	n_D^b	$\Delta R/\text{cm}^3 \text{mol}^{-1}$
298.2 K				
0.0509	1.12872	0.0031	1.4343	-0.0071
0.0999	1.13268	0.0063	1.4333	-0.0213
0.2004	1.14067	0.0114	1.4316	-0.0369
0.2999	1.14847	0.0150	1.4300	-0.0476
0.3999	1.15614	0.0170	1.4284	-0.0537
0.4999	1.16367	0.0176	1.4268	-0.0546
0.5972	1.17087	0.0167	1.4254	-0.0508
0.6999	1.17832	0.0152	1.4239	-0.0423
0.7998	1.18544	0.0119	1.4225	-0.0312
0.8997	1.19244	0.0070	1.4211	-0.0150
0.9498	1.19591	0.0034	1.4204	-0.0046
308.2 K				
0.0500	1.11882	0.0031	1.4302	-0.0112
0.1015	1.12293	0.0068	1.4292	-0.0238
0.2016	1.13081	0.0132	1.4275	-0.0396
0.3001	1.13842	0.0177	1.4259	-0.0487
0.4004	1.14602	0.0208	1.4244	-0.0545
0.4993	1.15339	0.0218	1.4228	-0.0562
0.6002	1.16076	0.0213	1.4213	-0.0520
0.6997	1.16790	0.0194	1.4199	-0.0437
0.7989	1.17492	0.0145	1.4185	-0.0345
0.9001	1.18195	0.0088	1.4171	-0.0161
0.9442	1.18499	0.0044	1.4165	-0.0082
318.2 K				
0.0511	1.10906	0.0041	1.4258	-0.0069
0.1017	1.11305	0.0085	1.4250	-0.0160
0.2018	1.12084	0.0149	1.4234	-0.0293
0.2979	1.12817	0.0202	1.4218	-0.0415
0.4021	1.13598	0.0235	1.4202	-0.0493
0.5000	1.14319	0.0245	1.4187	-0.0512
0.5980	1.15029	0.0236	1.4173	-0.0484
0.7001	1.15753	0.0220	1.4159	-0.0398
0.8009	1.16458	0.0173	1.4145	-0.0262
0.8992	1.17134	0.0108	1.4132	-0.0124
0.9491	1.17473	0.0068	1.4125	-0.0059

^aStandard uncertainties u are $u(x)=0.0001$, $u(\rho)=6\times 10^{-5} \text{ g}\cdot\text{cm}^{-3}$, $u(T)=0.01 \text{ K}$

^bStandard uncertainties u are $u(n_D)=1.5\times 10^{-4}$, $u(T)=0.05 \text{ K}$

$$V^E/\text{cm}^3 \cdot \text{mol}^{-1} = \frac{\sum_i x_i M_i}{\rho_m} - \sum_i \left[\frac{x_i M_i}{\rho_i} \right] \quad (7)$$

where x_i , M_i , ρ_i and ρ_m represent the mole fraction, the molecular weight, and the directly measured density of the pure component i and the binary mixture, respectively. In addition, the deviations of refractive indices, ΔR , were calculated from Eq. (8) using the molar refractivity of pure and mixed components and volume fraction of the component [31,32]:

Table 8. Kinematic viscosities, and deviations for diethyl carbonate (1)+ γ -butyrolactone(2) binary systems at 298.2-318.2 K

x_1	$\nu/\text{mm}^2\cdot\text{s}^{-1}$	$\Delta\nu/\text{mm}^2\cdot\text{s}^{-1}$	x_1	$\nu/\text{mm}^2\cdot\text{s}^{-1}$	$\Delta\nu/\text{mm}^2\cdot\text{s}^{-1}$
298.2 K					
0.0499	1.408	-0.0210	0.6002	0.949	-0.0776
0.1000	1.350	-0.0425	0.6996	0.890	-0.0645
0.2001	1.254	-0.0658	0.8001	0.837	-0.0438
0.3000	1.169	-0.0772	0.9001	0.786	-0.0216
0.4000	1.090	-0.0831	0.9501	0.762	-0.0085
0.5001	1.017	-0.0833	-	-	-
308.2 K					
0.0499	1.225	-0.0181	0.6002	0.841	-0.0613
0.1000	1.176	-0.0365	0.6996	0.789	-0.0522
0.2001	1.094	-0.0558	0.8001	0.741	-0.0376
0.3000	1.025	-0.0633	0.9001	0.700	-0.0168
0.4000	0.959	-0.0674	0.9501	0.680	-0.0064
0.5001	0.897	-0.0671	-	-	-
318.2 K					
0.0499	1.075	-0.0122	0.6002	0.748	-0.0522
0.1000	1.035	-0.0267	0.6996	0.707	-0.0408
0.2001	0.962	-0.0474	0.8001	0.666	-0.0299
0.3000	0.899	-0.0575	0.9001	0.627	-0.0162
0.4000	0.844	-0.0610	0.9501	0.611	-0.0065
0.5001	0.792	-0.0606	-	-	-

Standard uncertainties u are $u(\nu)=0.001\text{ mm}^2\cdot\text{s}^{-1}$, $u(T)=0.01\text{ K}$. The range of the Ubbelohde viscometer utilized in this experiment was approximately 0.5 to $3\text{ mm}^2\cdot\text{s}^{-1}$

$$\Delta R/\text{cm}^3\cdot\text{mol}^{-1}=R_m-\sum_i\phi_iR_i \quad (8)$$

$$R_m=\left[\frac{n_D^2-1}{n_D^2+1}\right]\left[\frac{\sum_i x_i M_i}{\rho_m}\right] \quad (9)$$

$$R_i=\left[\frac{n_{D,i}^2-1}{n_{D,i}^2+1}\right]\left[\frac{M_i}{\rho_i}\right] \quad (10)$$

$$\phi_i=\frac{x_i V_i}{\sum_j x_j V_j} \quad (11)$$

where R_m , R_i , ϕ_i , n_D , $n_{D,i}$ and V_i represent the molar refractivity of mixture and pure component i , volume fraction of the pure component i in the mixture, the refractive index of the mixture and the pure component i and the molar volume of the pure component i , respectively.

The deviation of kinematic viscosity, $\Delta\nu$ values was also determined for the binary mixtures from the measured kinematic viscosity using following Eq. (12):

$$\Delta\nu/\text{mm}^2\cdot\text{s}^{-1}=\nu-\sum_i\nu_i x_i \quad (12)$$

where ν , ν_i represent the experimentally determined kinematic viscosity of the mixture and pure component i in the mixture. The Redlich-Kister model [14,33] was used to correlate the determined V^E , ΔR , and $\Delta\nu$ values, which is presented in Eq. (13)

Table 9. Kinematic viscosities, and deviations for propylene carbonate(1)+ γ -butyrolactone(2) binary systems at 298.2-318.2 K

x_1	$\nu/\text{mm}^2\cdot\text{s}^{-1}$	$\Delta\nu/\text{mm}^2\cdot\text{s}^{-1}$	x_1	$\nu/\text{mm}^2\cdot\text{s}^{-1}$	$\Delta\nu/\text{mm}^2\cdot\text{s}^{-1}$
298.2 K					
0.0500	1.485	-0.0068	0.5999	1.727	-0.0471
0.1000	1.502	-0.0150	0.7000	1.787	-0.0385
0.2000	1.540	-0.0283	0.8000	1.851	-0.0252
0.2998	1.579	-0.0405	0.8999	1.915	-0.0125
0.4000	1.623	-0.0486	0.9501	1.948	-0.0060
0.5001	1.672	-0.0503	-	-	-
308.2 K					
0.0500	1.289	-0.0044	0.5999	1.479	-0.0266
0.1000	1.303	-0.0092	0.7000	1.522	-0.0217
0.2000	1.333	-0.0181	0.8000	1.567	-0.0157
0.2998	1.365	-0.0248	0.8999	1.611	-0.0097
0.4000	1.401	-0.0276	0.9501	1.636	-0.0041
0.5001	1.437	-0.0294	-	-	-
318.2 K					
0.0500	1.127	-0.0017	0.5999	1.282	-0.0108
0.1000	1.140	-0.0034	0.7000	1.313	-0.0092
0.2000	1.167	-0.0065	0.8000	1.345	-0.0071
0.2998	1.194	-0.0095	0.8999	1.378	-0.0037
0.4000	1.222	-0.0111	0.9501	1.395	-0.0018
0.5001	1.251	-0.0118	-	-	-

Standard uncertainties u are $u(\nu)=0.001\text{ mm}^2\cdot\text{s}^{-1}$, $u(T)=0.01\text{ K}$. The range of the Ubbelohde viscometer utilized in this experiment was approximately 0.5 to $3\text{ mm}^2\cdot\text{s}^{-1}$.

$$V^E, \Delta R \text{ or } \Delta\nu=x_1 x_2 \sum_{i=1}^n A_i (x_1-x_2)^{i-1} \quad (13)$$

where x is the mole fraction, A_i is fitted Redlich-Kister parameter and n signifies a number of parameters. The optimal values of the parameters were determined by following the Akaike Information Criterion (AIC) [34], which is as follows:

$$\text{AIC}=N \ln \text{SR}+2 \quad (14)$$

where N denotes the number of data points, SR is sum of squares of residuals, and n is the number of parameters. We considered only less than seven parameters for convenient application in the engineering field and decided the numbers of parameter that produced the smallest AIC value [35].

The determined V^E values are plotted in Fig. 4 and 5. The solid lines, which indicate the calculated values of V^E with the Redlich-Kister parameters, are agreed very well with the experimental V^E data of each mixture, as shown in the figures. The mean deviations of the V^E values, for the {DEC(1)+GBL(2)} system, between the experimental and calculated data are 0.0016, 0.0082, and $0.0024\text{ cm}^3\text{ mol}^{-1}$ for 298.2, 308.2, and 318.2 K, respectively. The {PC(1)+GBL(2)} system showed a much smaller deviation than the {DEC(1)+GBL(2)} system, namely 0.0002, 0.0004, and $0.0003\text{ cm}^3\text{ mol}^{-1}$ at 298.2, 308.2, and 318.2 K, respectively. The V^E values of the {DEC(1)+GBL(2)} binary mixture negatively deviate from ideal behavior in the whole composition range for all the experi-

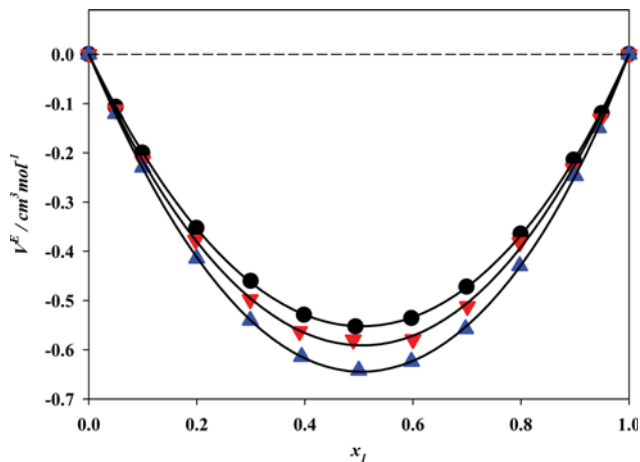


Fig. 4. V^E ($\text{cm}^3 \cdot \text{mol}^{-1}$) for {DEC(1)+GBL(2)} binary systems; (●), 298.2 K; (▼), 308.2 K; (▲), 318.2 K; solid curves were calculated from Redlich-Kister parameters.

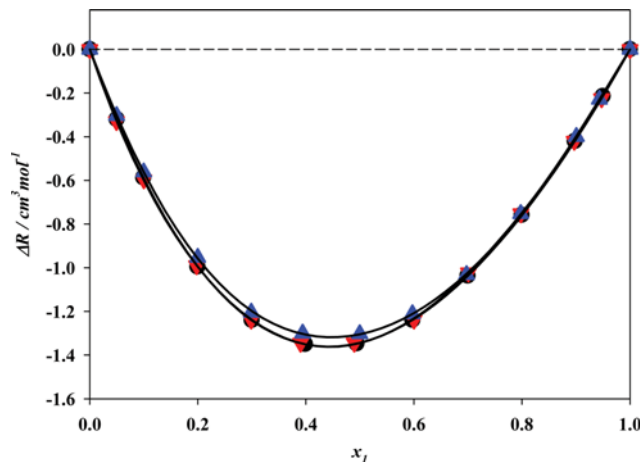


Fig. 6. ΔR ($\text{cm}^3 \cdot \text{mol}^{-1}$) for {DEC(1)+GBL(2)} binary systems; (●), 298.2 K; (▼), 308.2 K; (▲), 318.2 K; solid curves were calculated from Redlich-Kister parameters.

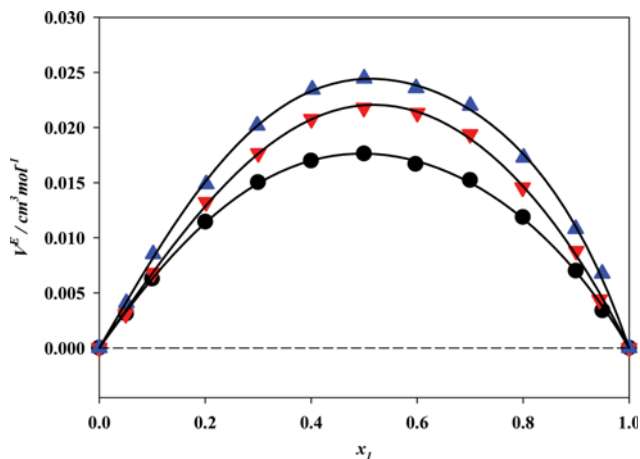


Fig. 5. V^E ($\text{cm}^3 \cdot \text{mol}^{-1}$) for {PC(1)+GBL(2)} binary systems; (●), 298.2 K; (▼), 308.2 K; (▲), 318.2 K; solid curves were calculated from Redlich-Kister parameters.

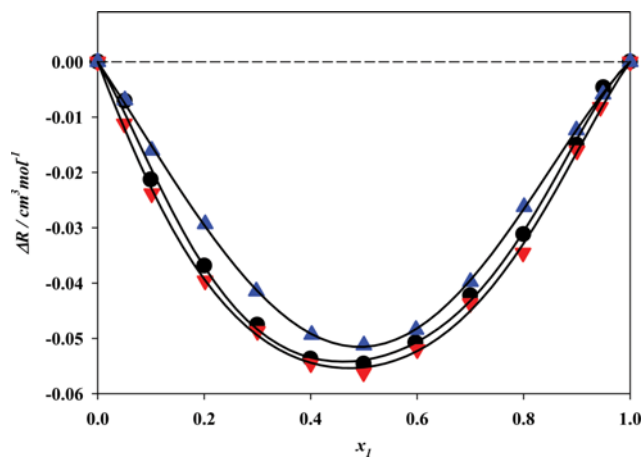


Fig. 7. ΔR ($\text{cm}^3 \cdot \text{mol}^{-1}$) for {PC(1)+GBL(2)} binary systems; (●), 298.2 K; (▼), 308.2 K; (▲), 318.2 K; solid curves were calculated from Redlich-Kister parameters.

mental temperatures, as shown in Fig. 4. This negative deviation may be caused by the significant molecular interaction between GBL and DEC and the negativity of V^E were increased with increasing temperature. Actually, GBL has a large dipole moment of 4.27 ± 0.03 D, whereas that of DEC is 1.10 ± 0.06 . However, it supposed that the dipole-dipole interactions in GBL-DEC mixtures make mutual interaction and contribute to V^E negatively. In addition, the negative contribution to V^E originates from the geometrical fitting of unlike molecules, which have different molecular size and shape. Thus, it may be concluded that the geometrical fitting of unlike molecules and the strong hetero-molecular interaction, caused by dipole-dipole interactions between unlike polar molecules are fundamental reasons for negativity of V^E . Meanwhile, the {PC(1)+GBL(2)} system showed slightly positive values of V^E at the measured temperatures. PC is a polar liquid, which has a high molecular dipole moment of 4.9D but little or no specific association, and the electric constant of GBL is approximately 4.2D [36].

Despite the high polarity of PC and GBL, they exhibit positive V^E values for the entire range of concentration, even though their positive deviation from ideality was very small. Moreover, a systematic increase in V^E was noted with the rise in temperature. This positive V^E in the {PC(1)+GBL(2)} system may be discussed in terms of different molecular size and structures. Namely, the positive values of V^E can be visualized as being due to a closer approach of unlike molecules with a significantly different molar volume and the dispersion forces between two different molecules. Furthermore, the free volume effect caused by different structure of two molecules may also partly contribute to positive V^E values. Rather than being dependent on any difference in chemical nature, the difference in the free volume is due to the geometrical and structural differences between two different molecules.

The deviations of refractive indices, ΔR , from 298.15 K to 318.2 K, showed negative values over the whole ranges of composition, as shown in Figs. 6 and 7. Large negative deviations were calculated

for the system {DEC(1)+GBL(2)}, whereas that of the system {PC(1)+GBL(2)} was relatively very small. This is due to the behavior of the refractive index which is not highly nonlinear between pure components. There is no obvious temperature dependence for ΔR in the determined systems. The temperature dependence of ΔR value was not quite understandable over measured small temperature ranges, as can be seen in the Figures, i.e., the magnitude of the negativity was not a function of the system temperature. The negativity of the {DEC(1)+GBL(2)} system is much larger than that of the system {PC(1)+GBL(2)}, and this may be caused by the size of the molar volumes of DEC (ca. 121.2 ml) and PC (ca. 76.3 ml) with GBL (ca. 76.3 ml). In addition, the intermolecular interaction between unlike molecules of the {DEC(1)+GBL(2)} system was much larger than for the {PC(1)+GBL(2)} system. By the way, the molar refractivity of the liquid mixture would be a function of not only interactions between molecules but also a molecular structure [37]. As can be seen in the figures of V^E and ΔR for the same systems, ΔR values showed different phenomena compared to the V^E deviation. In general, the negative deviations in ΔR were considered to be due to the presence of significant interactions between the components of a mixture [38,39]. The mean deviations of ΔR by the Redlich-Kister correlation were 0.0015, 0.0046, and 0.0066 at 298.2, 308.2, and 318.2 K for the {DEC(1)+GBL(2)} system, respectively, whereas the corresponding values of the system {PC(1)+GBL(2)} were 0.0018, 0.0012, and 0.0005 $\text{cm}^3 \cdot \text{mol}^{-1}$ at 298.2, 308.2, and 318.2 K, respectively.

In the case of deviations of the kinematic viscosity, $\Delta \nu$, for both binary systems, there were negative deviations for all the measured temperature ranges. The viscosity deviations of the liquid mixture may be generally explained by the difference in size and shape of the component molecules and the loss of dipolar association to the decrease in viscosity [40]. Usually, positive values are caused by strong interactions, whereas negative values come from weaker interactions or specific interactions. As shown in Figs. 8 and 9, the deviation of the {PC(1)+GBL(2)} system is more negative than that of {DEC(1)+GBL(2)}, since the {PC(1)+GBL(2)} system showed a weaker interaction than that of the {DEC(1)+

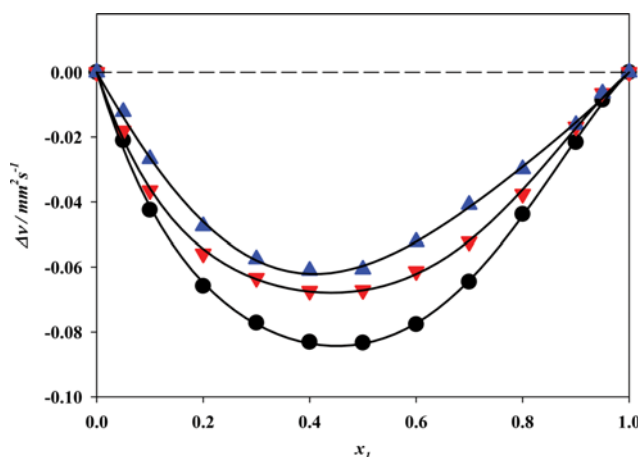


Fig. 8. $\Delta \nu$ ($\text{mm}^2 \cdot \text{s}^{-1}$) for {DEC(1)+GBL(2)} binary systems; (●), 298.2 K; (▼), 308.2 K; (▲), 318.2 K; solid curves were calculated from Redlich-Kister parameters.

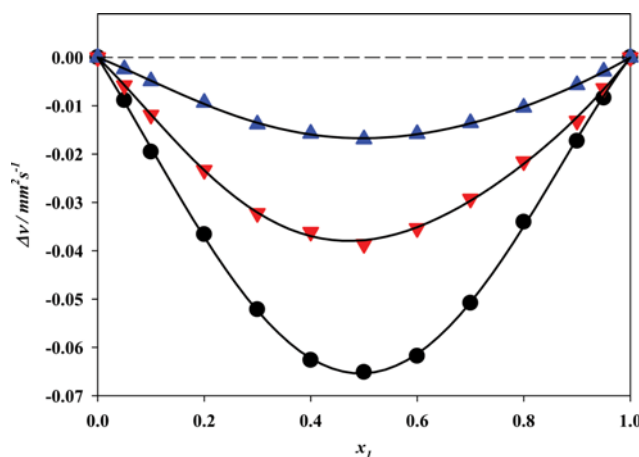


Fig. 9. $\Delta \nu$ ($\text{mm}^2 \cdot \text{s}^{-1}$) for {PC(1)+GBL(2)} binary systems; (●), 298.2 K; (▼), 308.2 K; (▲), 318.2 K; solid curves were calculated from Redlich-Kister parameters.

GBL(2)} system as seen in the V^E values of the {PC(1)+GBL(2)} system. As shown in Table 10 and Figs. 8 and 9, the Redlich-Kister correlation results were excellent. The mean standard deviations of the $\Delta \nu$ values for the {DEC(1)+GBL(2)} system were 0.0013, 0.0011, and 0.0014 $\text{mm}^2 \cdot \text{s}^{-1}$ at 298.2, 308.2, and 318.2 K, respectively. In contrast, the {PC(1)+GBL(2)} system showed a much smaller deviation than the {DEC(1)+GBL(2)} system, i.e., 0.0005, 0.0006, and 0.0001 $\text{mm}^2 \cdot \text{s}^{-1}$ at 298.2, 308.2, and 318.2 K, respectively.

3. Predictions of Density and Refractive Indices for the Binary Mixtures

The binary densities and refractive indices were predicted from some model equations and compared with the experimental values. In this work, the densities of the aforesaid two binary mixture systems, {DEC(1)+GBL(2)} and {PC(1)+GBL(2)}, were calculated using Nakata and Sakurai derived density prediction expression [41], in which the mixing rules for the refractive indices are expressed as functions of the volume fractions of the mixture. Eq. (15) is the Nakata and Sakurai expression, which uses the Lorentz-Lorenz [42] refractive index mixing rule:

$$\frac{\sum_i x_i M_i}{\rho} - \sum_i \frac{x_i M_i}{\rho_i} = - \left[\frac{6n_D}{(n_D^2 - 1)(n_D^2 + 2)} \right] \left[\sum_i \frac{x_i M_i}{\rho_i} \right] [n_D - (n_{D,1} \phi_1 + n_{D,2} \phi_2)] \quad (15)$$

where ρ and n_D are the binary mixture density and refractive index. $n_{D,1}$, $n_{D,2}$, ϕ_1 and ϕ_2 are the refractive index (n_D) and the volume fractions (ϕ) of pure components 1 and 2, respectively. M_i , ρ_i and x_i are the molar mass, density, and molar fraction of the pure component i , respectively. The absolute average deviation ($\Delta_{ADD}\%$) from the experimental data were calculated by using Eq. (16):

$$\Delta_{ADD}\% = \left(\frac{100}{N} \right) \sum_{i=1}^N \left| \frac{X_i^{exp} - X_i^{calc}}{X_i^{exp}} \right| \quad (16)$$

where X_i^{exp} and X_i^{calc} means the experimental and the calculated values, respectively. The prediction results of mixture density ac-

Table 10. Fitted parameters for the Redlich-Kister equation and standard deviations for V^E , ΔR and $\Delta \nu$ for the binary systems at 298.2–318.2 K

Systems			A_1	A_2	A_3	A_4	A_5	A_6	$\sigma_{st}/\text{cm}^3 \text{mol}^{-1}$
DEC(1) + GBL(2)	298.2 K	V^E	-2.2175	-0.0826	0.0145	0.1886	-0.2305	-0.2970	0.0016
		ΔR	-5.3749	1.2267	-0.3044	-	-	-	0.0015
		$\Delta \nu$	-0.3343	0.0595	-0.0180	0.1304	-	-	0.0013
	308.2 K	V^E	-2.3853	-0.0574	-	-	-	-	0.0082
		ΔR	-5.3800	1.2319	-0.0147	0.1586	-0.5061	-	0.0046
		$\Delta \nu$	-0.2647	0.0510	-0.1063	0.1222	0.1081	-	0.0011
318.2 K	V^E	-2.5787	-0.0482	-0.1344	-0.1022	-	-	0.0024	
	ΔR	-5.2358	1.0863	-0.2179	-	-	-	0.0066	
	$\Delta \nu$	-0.2370	0.0882	-	-	-	-	0.0014	
PC(1) + GBL(2)	298.2 K	V^E	0.0699	-0.0010	0.0152	0.0083	-0.0180	-	0.0002
		ΔR	-0.2204	0.0332	0.0433	-	-	-	0.0018
		$\Delta \nu$	-0.2016	0.0149	0.0848	-	-	-	0.0005
	308.2 K	V^E	0.0872	0.0095	-	-	-	-	0.0004
		ΔR	-0.2227	0.0340	-	-	-	-	0.0012
		$\Delta \nu$	-0.1150	0.0206	0.0235	-0.0293	-	-	0.0006
318.2 K	V^E	0.0976	0.0043	0.0127	0.0248	-	-	0.0003	
	ΔR	-0.2062	0.0149	0.0853	-	-	-	0.0005	
	$\Delta \nu$	-0.0464	0.0057	0.0113	-0.0345	-0.0001	0.0326	0.0001	

Table 11. Absolute average deviation ($\Delta_{ADD}\%$) in the calculation of the densities and refractive indices using the different equations: Nakata-Sakurai (N-S), Lorentz-Lorenz (L-L), Gladstone-Dale (G-D) Weiner (W), Heller (H)

Binary systems		β	n_D $\Delta_{ADD}\%$				
		$\Delta_{ADD}\%$	N-S	L-L	G-D	W	H
DEC(1)	298.2 K	0.0444	0.0953	0.0860	0.0895	0.0970	
+	308.2 K	0.0225	0.1087	0.0992	0.1028	0.1105	
GBL(2)	318.2 K	0.0894	0.1515	0.1420	0.1455	0.1533	
PC(1)	298.2 K	0.0071	0.0036	0.0042	0.0040	0.0039	
+	308.2 K	0.0059	0.0051	0.0058	0.0056	0.0052	
GBL(2)	318.2 K	0.0189	0.0028	0.0029	0.0028	0.0032	

According to the temperatures are reported in terms of the $\Delta_{ADD}\%$ in Table 11. They are also plotted in Fig. 10. As shown, the agreement between the predicted and experimental values is very good.

On the other hand, the predictions of the binary mixture refractive indices are also based on the mixing theories. In this work, the binary mixture refractive indices were predicted using the mixing rules proposed by Lorentz-Lorenz [42], Gladstone-Dale [43], Weiner [44], and Heller [45]. Their corresponding equations are as follows in order:

$$\frac{n_D^2 - 1}{n_D^2 + 2} = \sum_{i=1}^2 \phi_i \left[\frac{n_{D,i}^2 - 1}{n_{D,i}^2 + 2} \right] \quad (17)$$

$$n_D - 1 = \sum_{i=1}^2 \phi_i (n_{D,i} - 1) \quad (18)$$

$$\frac{n_D^2 - n_{D,1}^2}{n_D^2 + 2n_{D,1}^2} = \phi_2 \left[\frac{n_{D,2}^2 - n_{D,1}^2}{n_{D,2}^2 + 2n_{D,1}^2} \right] \quad (19)$$

$$\frac{n_D - n_{D,1}}{n_{D,1}} = \frac{3}{2} \phi_2 \left[\frac{\left(\frac{n_{D,2}}{n_{D,1}} \right)^2 - 1}{\left(\frac{n_{D,2}}{n_{D,1}} \right)^2 + 2} \right] \quad (20)$$

In these equations, n_D , $n_{D,i}$ and ϕ_i are the refractive indices of the mixture, the pure component i , and the volume fraction of component i , respectively. The absolute average deviation, $\Delta_{ADD}\%$ for refractive indices predictions was calculated using Eq. (16) and also given in Table 11 and plotted in Fig. 11. As shown, unlike the {PC(1)+GBL(2)} system, the predicted values for the {DEC(1)+GBL(2)} system are slightly lower than the experimental values over the entire region of concentrations and measured temperatures. However, the values of $\Delta_{ADD}\%$ were less than ca. 0.15% for all the binary systems.

CONCLUSIONS

The temperature dependency of the densities, refractive indices, kinetic viscosities, and excess and deviation properties of the GBL-containing solvent mixtures of lithium ion batteries were determined. The determined physical properties of the pure components decreased with increasing temperature. Most of the determined pure component densities, refractive indices, and kinetic viscosities were well correlated with the values calculated with the DIPPR, linear, and Goletz and Tassion equations within a deviation of ca. 0.1%, respectively.

The values of V^E were found to be negative for the {DEC(1)+GBL(2)} system and positive for the {PC(1)+GBL(2)} system, whereas ΔR and $\Delta \nu$ showed negative values for all temperatures and the whole composition ranges for both systems. These results were discussed in the light of the intermolecular interaction and molec-

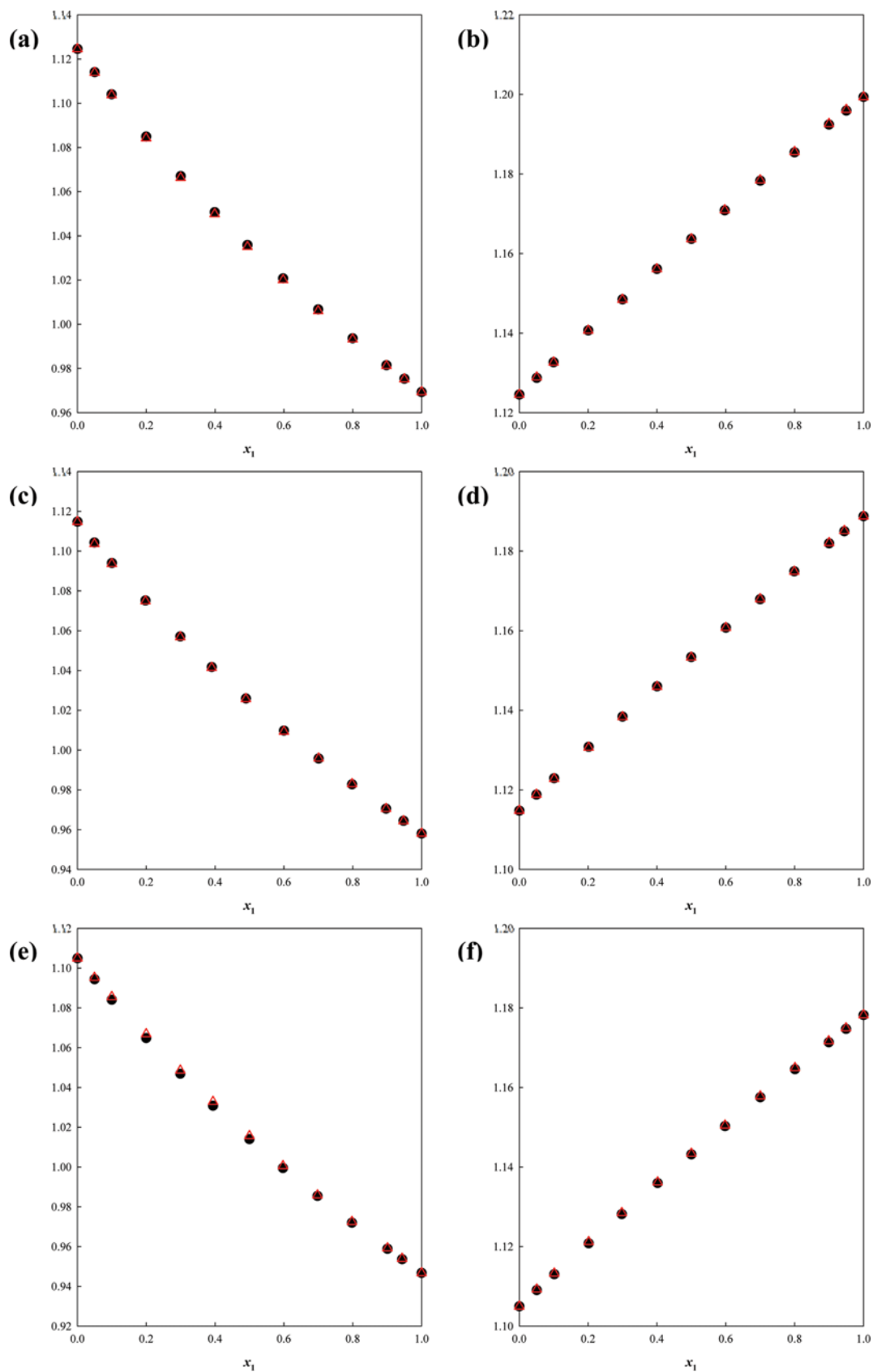


Fig. 10. Densities, $\rho/\text{g}\cdot\text{cm}^{-3}$, for the binary systems. (a) {DEC+GBL} at 298.2 K, (b) {PC+GBL} at 298.2 K, (c) {DEC+GBL} at 308.2 K, (d) {PC+GBL} at 308.2 K (e) {DEC+GBL} at 318.2 K, (f) {PC+GBL} at 318.2 K. ●, Experimental data; △, data calculated using the Lorentz-Lorenz equation.

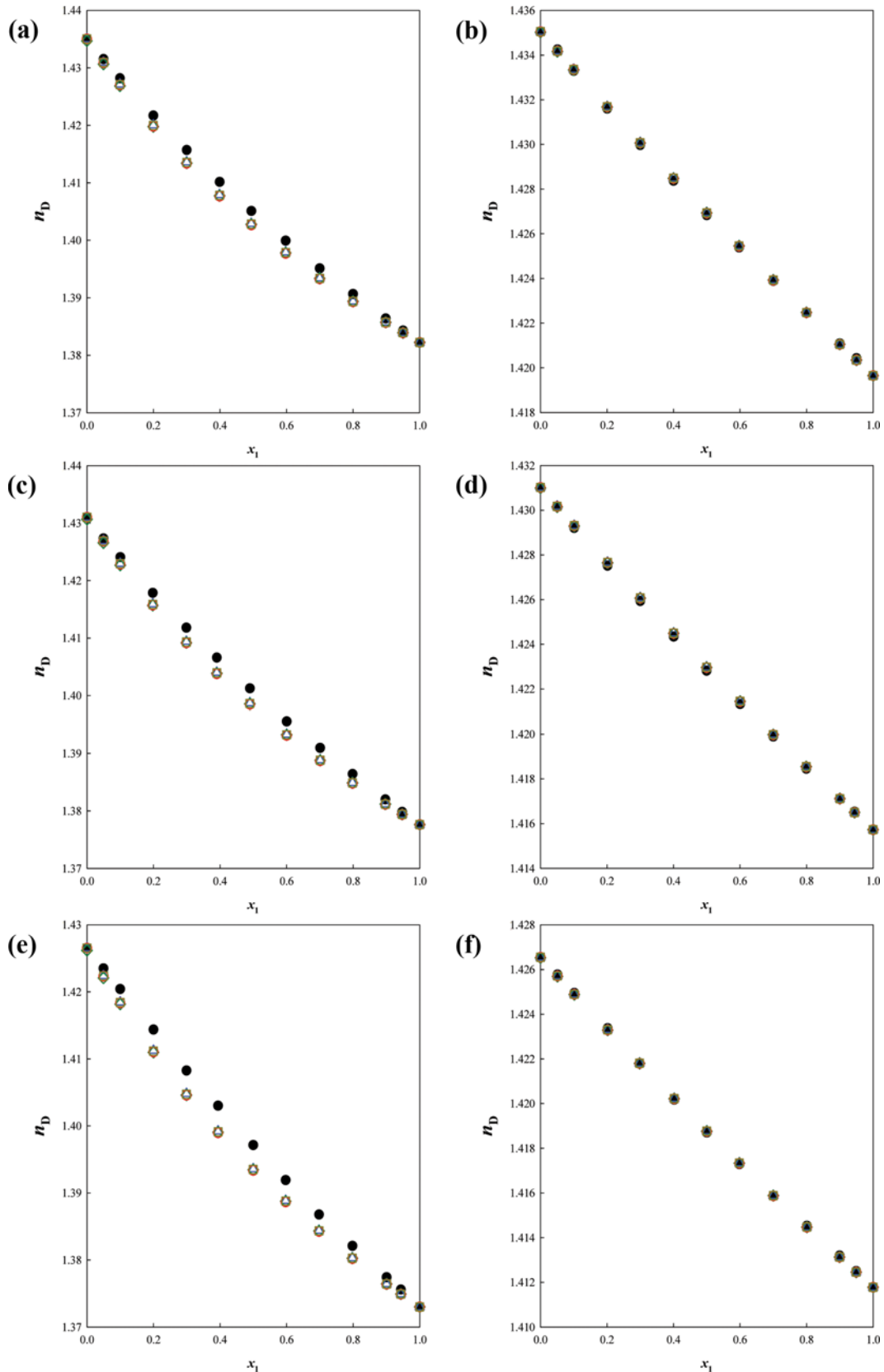


Fig. 11. Refractive indices, n_D , for the binary systems. (a) {DEC+GBL} at 298.2 K, (b) {PC+GBL} at 298.2 K, (c) {DEC+GBL} at 308.2 K, (d) {PC+GBL} at 308.2 K (e) {DEC+GBL} at 318.2 K, (f) {PC+GBL} at 318.2 K. ●, Experimental data; ○, data calculated using the Lorentz-lorenz equation; △, data calculated using the Gladstone-Dale equation; □, data calculated using the Wiener equation; ◇, data calculated using the Heller equation.

ular size and structure. The values of V^E and ΔV were shifted either negatively or positively in a regular way with increasing temperature. However, ΔR was not exactly dependent on the temperature over the determined small temperature ranges. They were correlated very well with Redlich-Kister polynomials within ca. 0.008 of standard deviation. Predictions of the binary mixture density and the refractive indices were made by using various equations. A comparison of the densities of the mixtures showed that they were in good agreement within an absolute average deviation of 0.09%. In the case of refractive indices for the mixtures, contrary to the {PC(1)+GBL(2)} system, the predictive values for the {DEC(1)+GBL(2)} system were slightly lower than the experimental values for the entire concentration region. However, the absolute average deviation was less than ca. 0.15%.

ACKNOWLEDGEMENTS

This work was supported by the research fund of Chungnam National University.

REFERENCES

- J. Dang, F. Xiang, N. Gu, R. Zhang, R. Mukherjee, I. Oh, N. Koratkar and Z. Yang, *J. Power Sources*, **243**, 33 (2013).
- L. Shen, H. Li, E. Uchaker, X. Zhang and G. Cao, *Nano Lett.*, **12**, 5673 (2012).
- L. Xing, W. Le, C. Wang, F. Gu, M. Xu, C. Tan and J. Yi, *J. Phys. Chem.*, **113**, 16596 (2009).
- H. Nithya, S. Selvasekarapandian, P.C. Selvin, D.A. Kumar and M. Hema, *Ionics*, **17**, 587 (2011).
- S. J. Pai and Y. C. Bae, *Fluid Phase Equilib.*, **332**, 94 (2012).
- N. Hafaiiedh, A. Toumi and M. Bouanz, *Phys. Chem. Liq.*, **47**, 399 (2009).
- F. Chen, Z. Yang, Z. Chen, J. Hu, C. Chen and J. Cai, *J. Mol. Liq.*, **209**, 683 (2015).
- G. Ritzoulis, D. Missopolinou, S. Doulami and C. Panayiotou, *J. Chem. Eng. Data*, **45**, 636 (2000).
- H. Lu, J. Wang, Y. Zhao, X. Xuan and K. Zhuo, *J. Chem. Eng. Data*, **46**, 631 (2001).
- J. Huang, X. Liu, X. Kang, Z. Yu, T. Xu and W. Qiu, *J. Power Sources*, **189**, 458 (2009).
- L. Lorenzi, M. Fermeglia and G. Torriano, *J. Chem. Eng. Data*, **43**, 183 (1998).
- T. Daubert and R. Danner, *Physical and Thermodynamic Properties of Pure Chemicals*, Hemisphere Publishing Corp., New York (1989).
- E. Goletz and D. Tassions, *Ind. Eng. Chem. Process Des. Dev.*, **16**, 75 (1977).
- O. Redlich and A. Kister, *Ind. Eng. Chem.*, **40**, 345 (1948).
- M. Vranes, S. Papovic, A. Tot and N. Zec, *J. Chem. Thermodynamics*, **76**, 161 (2014).
- A. Farhan and A. Awwad, *J. Chem. Eng. Data*, **55**, 1035 (2010).
- C. Yang, W. Xu and P. Ma, *J. Chem. Eng. Data*, **49**, 1802 (2004).
- S.H. Shin, I.Y. Jeong, Y.S. Jeong and S.J. Park, *Fluid Phase Equilib.*, **376**, 105 (2014).
- C. Yang, H. Lai, Z. Liu and P. Ma, *J. Chem. Eng. Data*, **51**, 1345 (2006).
- A. Rodriguez, J. Canosa and J. Tojo, *J. Chem. Thermodynamics*, **35**, 1321 (2003).
- A. Naejus, D. Lemordant and R. Coudert, *J. Chem. Thermodynamics*, **29**, 1503 (1997).
- P. Sears, T. Stoeckinger and L. Dawson, *J. Chem. Eng. Data*, **16**, 220 (1971).
- M. Vranes, N. Zec, A. Tot, S. Papovic, S. Dozic and S. Gadzuric, *J. Chem. Thermodynamics*, **68**, 98 (2014).
- G. Moumouzias and G. Ritzoulis, *J. Chem. Eng. Data*, **45**, 202 (2000).
- I. Y. Jeong, R. H. Kwon, S. J. Park and Y. Y. Choi, *J. Chem. Eng. Data*, **59**, 289 (2014).
- K. H. Lee, S. J. Park and Y. Y. Choi, *Korean J. Chem. Eng.*, **34**, 214 (2017).
- S. Ottani, D. Vitalini, F. Comelli and C. Castellari, *J. Chem. Eng. Data*, **47**, 1197 (2002).
- J. Resa, C. Gonzalez and J. Goenaga, *J. Chem. Eng. Data*, **51**, 73 (2006).
- J. H. Oh and S. J. Park, *J. Chem. Eng. Data*, **43**, 1009 (1998).
- K. J. Han, J. H. Oh, S. J. Park and J. Gmehling, *J. Chem. Eng. Data*, **50**, 1951 (2005).
- T. Aminabhavi and B. Gopalakrishna, *J. Chem. Eng. Data*, **40**, 856 (1995).
- A. Al-Dujaili, A. Yassen and A. Awwad, *J. Chem. Eng. Data*, **45**, 647 (2000).
- D. Sen and M. G. Kim, *Korean J. Chem. Eng.*, **26**, 806 (2009).
- A. Akaike, *IEEE T. Automat. Contr.*, **19**, 716 (1974).
- L. Kirkup, *Data analysis with Excel*, Cambridge University Press: Cambridge (2002).
- D. Lide, *CRC Handbook of Chemistry and Physics*, 85th Ed., CRC Press (2004).
- W. Kauzmann and H. Eyring, *J. Am. Chem. Soc.*, **62**, 3113 (1940).
- P. Brocos, A. Pineiro, R. Bravo and A. Amigo, *Phys. Chem. Chem. Phys.*, **5**, 550 (2003).
- A. Nain, *J. Chem. Eng. Data*, **53**, 850 (2008).
- R. Maximino, *Phys. Chem. Liq.*, **47**, 515 (2009).
- M. Nakata and M. Sakurai, *J. Chem. Soc. Faraday Trans.*, **83**, 2449 (1987).
- H. Lorentz, *Ann. Phys.-Berlin*, **245**, 641 (1880).
- T. Dale and J. Gladstone, *Phil. Trans. R. Soc. Lond.*, **148**, 887 (1858).
- O. Wiener, *Zur theorie der Refraktionskonstanten*, Berichte über die Verhandlungen der Königlich-Sächsischen Gesellschaft der Wissenschaften zu Leipzig (1910).
- W. Heller, *J. Phys. Chem.*, **69**, 1123 (1965).